

ly, that of the highly visual tiger beetle larvae (18). However, in the strepsipteran eye no screening pigment appears to be present (22). The effective image resolution within each eyelet of *X. peckii* therefore depends not only on the number of photoreceptors but also on the extent of optical pooling, which remains to be further investigated. The image resolution would also be influenced by the degree of overlap between the visual fields of neighboring eyelets. The acceptance angle of an individual eyelet can be estimated if the focal length of the lens is known. On the basis of measurements of the image magnification (23), a focal length of $44 \pm 5 \mu\text{m}$ ($n = 21$) and an acceptance angle of $33^\circ \pm 6^\circ$ ($n = 10$) was calculated. Thus, the values for the acceptance angle are, if at all, only slightly greater than those of the inter-eyelet angle of $27^\circ \pm 6^\circ$. Our model (Fig. 4) assumes no overlap, but a small amount of overlap is conceivable and could be consistent with the unusual absence of clearly definable cartridges of the medulla.

For more than a century the arthropod eye has been extensively studied in structure and function, and many common features are conserved throughout this group. Although the detailed modes of function of arthropod eyes vary considerably (8), it is remarkable how profoundly the structural features of the eye of Strepsiptera have changed. The course of its evolution is unclear, but it is certainly noteworthy; after all, its organization may be a living counterpart to the eyes of some of the long-extinct trilobites.

References and Notes

1. R. K. Kinzelbach, in *Handbuch der Zoologie IV/2/2*, J. G. Helmcke, D. Starck, H. Wermuth, Eds. (de Gruyter, Berlin, ed. 2, 1971), pp. 1–68; K. Strohm, *Zool. Anz.* **36**, 156 (1910); P. Rösch, *Zeitschr. Naturwiss.* **50**, 97 (1913); H. F. Paulus, in *Arthropod Phylogeny*, A. P. Gupta, Ed. (Van Nostrand Reinhold, New York, 1979), pp. 299–383; H. R. MacCarthy, *J. Entomol. Soc. Brit. Columbia* **88**, 27 (1991).
2. Male *X. peckii* were collected as late pupae within their wasp hosts near Ithaca, NY.
3. The heads of late pupae and adults were stained with osmium or reduced silver. We estimated the number of rhabdoms (or functional receptor units) from light microscopy examination of sections of the retina.
4. D.-E. Nilsson, in *Facets of Vision*, D. G. Stavenga and R. C. Hardie, Eds. (Springer-Verlag, Berlin, 1989), pp. 30–73.
5. The back focal distance (distance between focal plane and the back of the lens) was measured with the hanging drop method, using a cover slip–corrected oil immersion lens, and corrected for the refractive index of immersion oil. For details see M. Wilson, *J. Comp. Physiol.* **124**, 297 (1978).
6. A. W. Snyder, *J. Comp. Physiol. A* **116**, 161 (1977); A. W. Snyder, D. G. Stavenga, S. B. Laughlin, *J. Comp. Physiol. A* **116**, 183 (1977).
7. G. A. Horridge, *Endeavour* **1**, 7 (1977).
8. M. F. Land, in *Handbook of Sensory Physiology VII/6B*, H. Autrum, Ed. (Springer-Verlag, Berlin, 1981), pp. 471–592.
9. The calculation is based on an average lens diameter of $65 \mu\text{m}$ and average inter-eyelet angle of 27° . Because there are on average 11 receptors across the diameter of the retina, the value for each receptor would be 2.8 ($31 \mu\text{m}/11$ receptors), a value that is

comparable to $D\Delta\Phi$ values of conventional compound eyes.

10. D. Fordyce and T. W. Cronin, *Paleobiology* **19**, 288 (1993).
11. The sensitivity [from (8)] was calculated as $S = (\pi/4)^2(A/f)^2d^2[1 - \exp(-kx)]$, where A is aperture ($65 \mu\text{m}$, measured), f is focal length ($44 \mu\text{m}$, calculated), d is receptor diameter ($1.5 \mu\text{m}$, estimated), x is receptor length ($11 \mu\text{m}$, measured), and k is the absorption coefficient. We used for k [like (8); see all invertebrates in table 5] the estimate of $0.0067 \mu\text{m}^{-1}$ based on measurements by M. S. Bruno, S. N. Barnes, T. H. Goldsmith, *J. Comp. Physiol. A* **120**, 123 (1977).
12. J. Meixner, in *Handbuch der Zoologie IV/2/2*, T. Krumbach, Ed. (de Gruyter, Berlin, ed. 1, 1936), pp. 1349–1382.
13. Retinal receptor terminals were stained by applying dextran molecules conjugated to fluorescein (molecular weight 3000, lysine-fixable; Molecular Probes) to individual eyelets and were viewed with a Bio-Rad 600 confocal microscope.
14. S. R. Cajal and D. Sánchez, *Trab. Lab. Invest. Biol. Univ. Madrid* **13**, 1 (1915).
15. Volumes were estimated by serial reconstruction. Outlines of neuropils were scanned in, measured in Adobe Photoshop, multiplied by section thickness, and the relative proportion of the summed volumes was calculated.
16. If each photoreceptor of *X. peckii* required its own lens, then the diameter of each lens would only be $6 \mu\text{m}$ ($65 \mu\text{m}/11$ receptors), resulting in a $D\Delta\Phi$ value

of 0.24, and therefore diffraction would be limiting (8). A single-lens eye with a wide field of view, however, requires a very short focal length for a small insect and thus a very thick lens, which usually has pronounced spherical and chromatic aberrations. Thus, pooling the information of a number of simple-lens eyes with a restricted field of view (“chunk sampling”) may be a good compromise.

17. E. J. Warrant and P. D. McIntyre, *Prog. Neurobiol.* **40**, 413 (1993).
18. Y. Toh and A. Mizutani, *Cell Tissue Res.* **278**, 125 (1994).
19. P. Duelli, *Cell Tissue Res.* **187**, 417 (1994); N. J. Strausfeld and F. G. Barth, *J. Comp. Neurol.* **328**, 43 (1993); N. J. Strausfeld, P. Weltzien, F. G. Barth, *J. Comp. Neurol.* **328**, 63 (1993).
20. M. F. Land, *J. Exp. Biol.* **51**, 443 (1969).
21. C. Gilbert, *Annu. Rev. Entomol.* **39**, 23 (1994).
22. E. Wachmann, *Z. Zellforsch.* **123**, 411 (1972).
23. The setup for image magnification measurements was as described in (5). The focal length f was calculated using the lens formula $O/U = l/f$, where O is object size, U is object distance, and l is image size. The acceptance angle is determined by f and the extension of the retina behind the lens.
24. We thank H. Bennet-Clark, C. Gilbert, W. Gronenberg, H. Howland, D. Papaj, W. Pix, J. Zeil, and all members of the Hoy lab for helpful discussions of the manuscript. M. Land and W. Zipfel provided advice regarding optical measurements. Supported by NIH and by the Deutsche Forschungsgemeinschaft.

19 July 1999; accepted 24 September 1999

Calmodulin Dependence of Presynaptic Metabotropic Glutamate Receptor Signaling

Vincent O'Connor,^{1*}† Oussama El Far,^{1*} Elisa Bofill-Cardona,² Christian Nanoff,² Michael Freissmuth,² Andreas Karschin,³ José M. Airas,¹ Heinrich Betz,^{1,‡} Stefan Boehm²

Glutamatergic neurotransmission is controlled by presynaptic metabotropic glutamate receptors (mGluRs). A subdomain in the intracellular carboxyl-terminal tail of group III mGluRs binds calmodulin and heterotrimeric guanosine triphosphate-binding protein (G protein) $\beta\gamma$ subunits in a mutually exclusive manner. Mutations interfering with calmodulin binding and calmodulin antagonists inhibit G protein-mediated modulation of ionic currents by mGluR 7. Calmodulin antagonists also prevent inhibition of excitatory neurotransmission via presynaptic mGluRs. These results reveal a novel mechanism of presynaptic modulation in which Ca^{2+} -calmodulin is required to release G protein $\beta\gamma$ subunits from the C-tail of group III mGluRs in order to mediate glutamatergic autoinhibition.

G protein-coupled receptors modulate ionic currents and exocytotic fusion reactions that underlie neurotransmitter release (1). Gluta-

mate release is controlled by presynaptic mGluRs inhibiting voltage-activated Ca^{2+} channels (2, 3) via G protein $\beta\gamma$ subunits (4). The selective localization of group III mGluRs at active zones is consistent with their predominant role as autoreceptors mediating feedback inhibition (5). The mGluRs show a heptahelical structure typical of G protein-coupled receptors (2, 6), and their COOH-terminal tails represent the major intracellular domain, which exhibits high variation among receptor subclasses (2). We chose this region to investigate interacting proteins that might contribute to the functional diversity of mGluRs.

¹Department of Neurochemistry, Max Planck Institute for Brain Research, Deutschordenstrasse 46, 60528 Frankfurt, Germany. ²Institute of Pharmacology, University of Vienna, Währingerstrasse 13a, 1090 Vienna, Austria. ³Molecular Neurobiology of Signal Transduction, Max Planck Institute for Biophysical Chemistry, 37070 Göttingen, Germany.

*These authors contributed equally to this report. †Present address: University of Southampton, Biomedical Sciences Building, Basset Crescent East, Southampton SO16 7PX, UK.

‡To whom correspondence should be addressed. E-mail: neurochemie@mpih-frankfurt.mpg.de

REPORTS

Mouse brain cDNA was used to amplify (7) the sequence encoding the C-tail of the group III receptor 7. The variant C-tails, m-7A and m-7B (Fig. 1A), were expressed as recombinant proteins fused to glutathione S-

transferase (GST) and used in an affinity purification procedure (8) from rat brain extract (Fig. 1B). Comparison of Coomassie blue-stained gel lanes with parallel samples obtained with immobilized GST indicated

that an 18-kD protein bound specifically to both GST-7A (Fig. 1B) and GST-7B that was not stained with silver (Fig. 1C). Poor reactivity toward silver is associated with acidic proteins; immunostaining identified the 18-kD band as calmodulin (molecular mass 18 kD; $pI \approx 4$), a Ca^{2+} sensor protein (9) known to bind to mGluR 5 (10). Purification in the presence of Ca^{2+} or of EGTA revealed that calmodulin binding to both GST-7A and GST-7B was Ca^{2+} dependent (Fig. 1D). The binding of calmodulin occurred at <100 nM Ca^{2+} and with a dissociation constant K_D of 57 nM at saturating Ca^{2+} concentrations (11).

The interaction between Ca^{2+} -calmodulin and the C-tail of mGluR 7 was confirmed in binary binding assays (8) with immobilized fusion proteins and purified calmodulin. A fusion protein encompassing the 27 COOH-terminal amino acids of mGluR 7A (C27; see Fig. 1A) failed to bind calmodulin, but fusion constructs N38 and N25 containing the common NH_2 -terminal fragments (Fig. 1A) both bound calmodulin (12). The 25 amino acids of N25 are highly conserved in all members of group III but not other mGluRs and display homology to a consensus calmodulin binding sequence (13). Calmodulin binding to GST-7A was fully prevented by the irreversible calmodulin antagonist ophiobolin A (12, 14). Also, mGluR 7 solubilized from rat hippocampal synaptosomes bound to Ca^{2+} -calmodulin immobilized on agarose beads, thus confirming binding of Ca^{2+} -calmodulin by a native group III mGluR (15).

The tail regions of heptahelical receptors contribute to G protein coupling. We therefore examined whether binding of calmodulin to mGluR 7 might interfere with its interaction with trimeric G protein subunits. When detergent extracts of porcine brain membranes were used in pull-down experiments with immobilized GST-7A (16), a band migrating at ~ 35 kD was retained and recognized by an antiserum to G protein β subunits

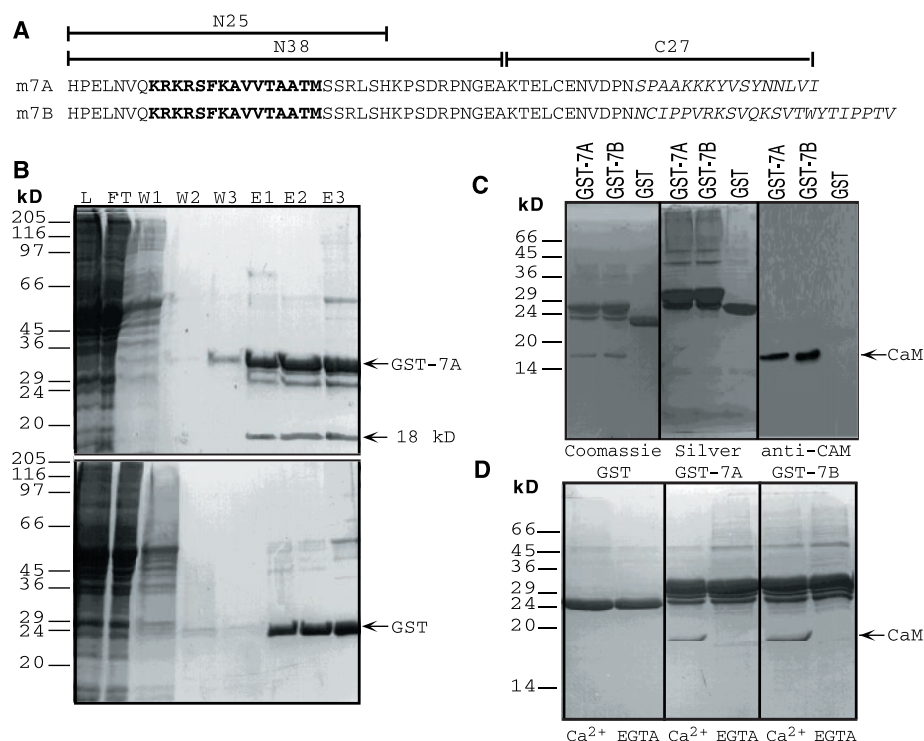
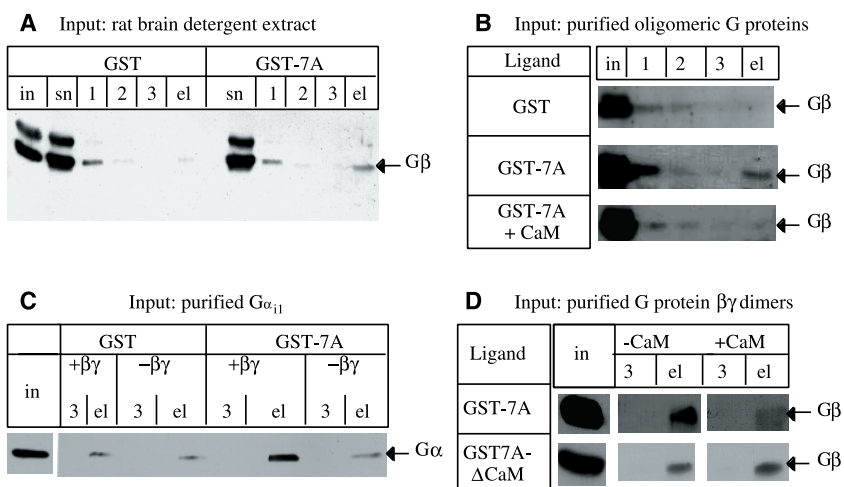


Fig. 1. A Ca^{2+} -dependent calmodulin binding site exists on the C-tails of mGluR 7 splice variants. **(A)** Alignment of the mGluR 7A and 7B tail sequences. Partial mGluR 7A sequences used in pull-down experiments are indicated by bars. Italic characters represent regions of alternative splicing; bold characters indicate the potential calmodulin binding domain. **(B)** The C-tail of mGluR 7A fused to GST (GST-7A; top) and GST alone (bottom) were immobilized on glutathione-Sepharose and incubated with a cytosolic extract of rat brain (lane L). After collection of the flow-through (lane FT) and sequential washes (lanes W1 to W3), bound proteins were sequentially eluted with 15 mM glutathione (lanes E1 and E2) and SDS-PAGE sample buffer (lane E3). SDS-PAGE revealed that GST-7A, but not GST, bound an 18-kD protein. **(C)** Brain cytosolic proteins bound to GST-7A or GST-7B were eluted with SDS-PAGE sample buffer and analyzed by Coomassie blue and silver staining. Note that the 18-kD band revealed by Coomassie staining was not stained by silver. Protein immunoblotting identified the 18-kD copurifying protein as calmodulin (CaM). **(D)** Incubating rat brain cytosolic proteins with GST, GST-7A, or GST-7B in the presence of $CaCl_2$ (1 mM) or EGTA (5 mM) revealed that the binding of calmodulin to the mGluR 7 tail regions is Ca^{2+} -dependent. The experiments shown in (B) to (D) were performed 2 to 10 times.

Fig. 2. Binding of $G\beta\gamma$ to the C-tail of mGluR 7A. **(A)** A CHAPS extract of porcine brain membranes (input = lane in) was incubated with the mGluR 7A tail region (GST-7A) or GST. Unbound proteins were recovered in the supernatant (lanes sn); after three washes (lanes 1 to 3), bound proteins were eluted with 30 mM glutathione (lanes el). Equal fraction volumes were subjected to SDS-PAGE and protein immunoblotting with a mixture of antisera to $G\alpha$ and $G\beta$. **(B)** Interaction between purified oligomeric G proteins (30 pmol) and GST-7A or GST in the presence (+CaM) and absence of Ca^{2+} and calmodulin. For conditions and lane labels, see (A). **(C)** Binding of purified recombinant $G\alpha_{i1}$ (60 pmol) to GST or GST-7A in the presence (+ $\beta\gamma$) and absence (- $\beta\gamma$) of $G\beta\gamma$ dimers (120 pmol). **(D)** Binding of purified $G\beta\gamma$ (30 pmol) to GST-7A and GST-7A- Δ CaM in the absence (-CaM) and presence (+CaM) of Ca^{2+} and calmodulin. In (C) and (D), only the input (in), third wash (3), and elution (el) lanes are shown. All data were corroborated in three to five separate experiments.



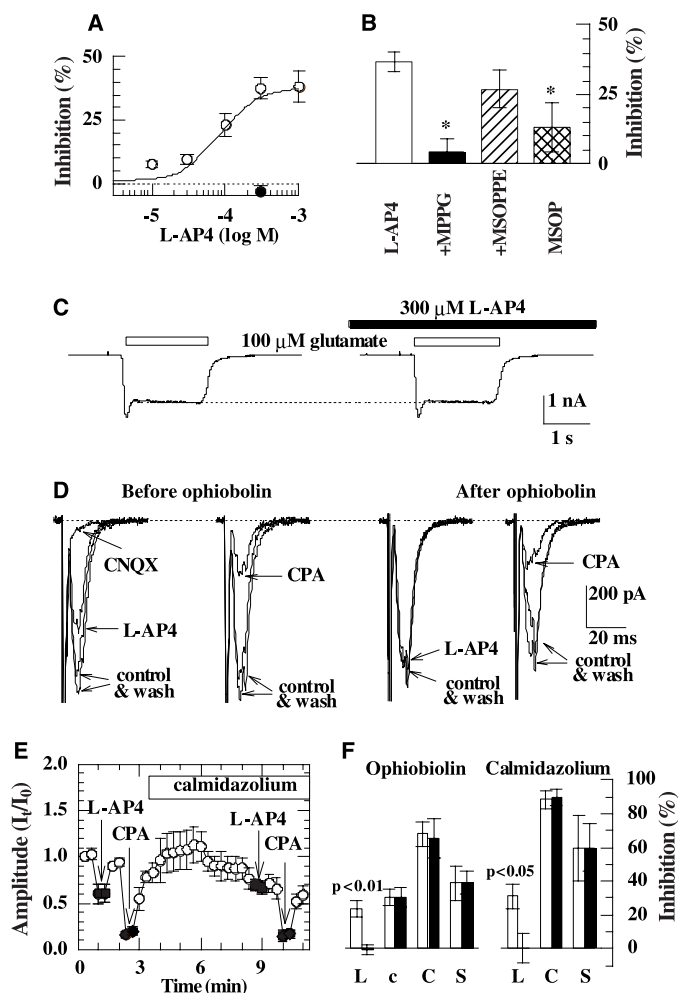
REPORTS

(G β) (Fig. 2A). In contrast, only trace amounts of G protein α subunits (G α) were detected. A specific interaction with G protein $\beta\gamma$ dimers (G $\beta\gamma$) was confirmed using purified proteins (16). Because group III mGluRs signal via pertussis toxin-sensitive G proteins (2, 17), we tested binding with a mixture of heterotrimeric G $_i$ and G $_o$. GST-7A, but not GST, bound the β subunit (Fig. 2B). G $\beta\gamma$ chromatographically resolved from α subunits also associated with GST-7A (Fig. 2D). In contrast, GST-7A failed to specifically bind G α_i alone, but retained it in the presence of G $\beta\gamma$ (Fig. 2C). Furthermore, GST-7A did not accelerate the rate of guanosine 5'-O-(3'-triotriphosphate) (GTP- γ -S) binding to G α_{i1} in both the absence and the presence of $\beta\gamma$ dimers (18), which is consistent with the m-7A tail not contacting G α in the bound trimeric G protein. Ca $^{2+}$ -calmodulin inhibited the interaction between GST-7A and G $\beta\gamma$, regardless of whether incubations contained heterotrimeric G proteins (Fig. 2B) or $\beta\gamma$ dimers (Fig. 2D). Thus, binding of G $\beta\gamma$ and calmodulin is specific and mutually exclusive.

To assay transmitter release and its regulation by presynaptic receptors, we monitored autaptic currents of hippocampal neurons on micro-islands of glial cells (19, 20). The group III-selective mGluR agonist L-AP4 (6, 17) caused inhibition of glutamatergic (Fig. 3, A, B, and D), but not GABAergic (21), autaptic currents (GABA, γ -aminobutyric acid). This effect was not observed in cultures treated with pertussis toxin, indicating that L-AP4 activates G $_i$ /G $_o$ proteins (2, 17) (Fig. 3A). L-AP4 did not affect glutamate-evoked currents, consistent with its presynaptic action (Fig. 3C). Reverse transcription polymerase chain reaction (RT-PCR) analysis of RNA from cultured hippocampal neurons (12) corroborated the expression of group III mGluRs 4, 7A, 7B, and 8 in rat hippocampus (22). A concentration-response curve for the inhibition of glutamatergic transmission by L-AP4 revealed a median effective concentration of $60 \pm 18 \mu\text{M}$ (Fig. 3A). This inhibition was attenuated by the group III-prefering mGluR antagonists (*RS*)- α -methylserine-*O*-phosphate (MSOP) (23) and (*RS*)- α -methyl-4-phosphonophenylglycine (MPPG) (3), but not by (*RS*)- α -methylserine-*O*-phosphate monophenylphosphoryl ester (MSOPPE) (23), which preferentially blocks group II mGluRs (Fig. 3B); none of these antagonists had an effect when applied alone. Hence, L-AP4 inhibits glutamate release via group III mGluRs, with a predominant role of the low-affinity receptors mGluR 7A or 7B (17).

Exposure of neurons to the calmodulin antagonists ophiobolin A (14) or calmidazolium (24) abolished presynaptic inhibition by L-AP4 (Fig. 3, D and E). This effect was specific to mGluRs, because inhibition by somatostatin (Fig. 3F) or cyclopentylad-

Fig. 3. Presynaptic inhibition of glutamate release at hippocampal autapses by group III metabotropic glutamate receptors is attenuated selectively by calmodulin antagonists. (A) Concentration-response relation for the reduction of glutamatergic autaptic currents by L-AP4 [as shown in (D)] in either untreated neurons (\circ) or in neurons treated with pertussis toxin (100 ng/ml) for 24 hours (\bullet); $n = 4$ to 8. (B) Inhibitory action of 300 μM L-AP4 alone or in the presence of 100 μM MPPG, MSOPPE, or MSOP; $n = 5$ to 6 with the exception of L-AP4 alone, where $n = 17$; *, $p < 0.05$ versus L-AP4 alone (unpaired Student's *t* test). (C) Currents evoked by the direct application of 100 μM glutamate at a potential of -70 mV in the absence and presence of 300 μM L-AP4, respectively. Peak current amplitudes in the presence of 300 μM L-AP4 amounted to $103.2 \pm 3.0\%$ of those obtained in its absence; $n = 6$. (D) Reduction of autaptic currents in a glutamatergic micro-island neuron by 300 μM L-AP4 and 1 μM CPA, before and after a 3-min application of 25 μM ophiobolin A. In the left trace, the effect of the non-NMDA receptor antagonist CNQX (10 μM) is also shown. (E) Time course of normalized amplitudes of glutamatergic autaptic currents [as shown in (D)] in five neurons: 300 μM L-AP4 (\blacksquare) and 1 μM CPA (\blacklozenge) were applied during two consecutive stimulations (arrows), and 1 μM calmidazolium was present (bar). (F) Presynaptic inhibition caused by 300 μM L-AP4 (L), 0.01 μM (c) or 1 μM CPA (C), and 1 μM somatostatin (S) before (white bars) and after (black bars) 3-min applications of either 25 μM ophiobolin A [as shown in (D)] or 1 μM calmidazolium [as shown in (E)]; calmidazolium was also present during the second application of agonists; $n = 4$ to 10.



enosine (CPA; Fig. 3, D and F)—which act via presynaptic SRIF $_1$ (20) or A $_1$ (25) receptors, respectively—was not altered. Control experiments showed that L-AP4 (300 μM) had no significant effect on the average frequency and mean amplitude of miniature excitatory postsynaptic currents (MEPSCs), which occur independently of Ca $^{2+}$ entry, but significantly reduced the frequency of MEPSCs raised by depolarization with 10 mM KCl (21).

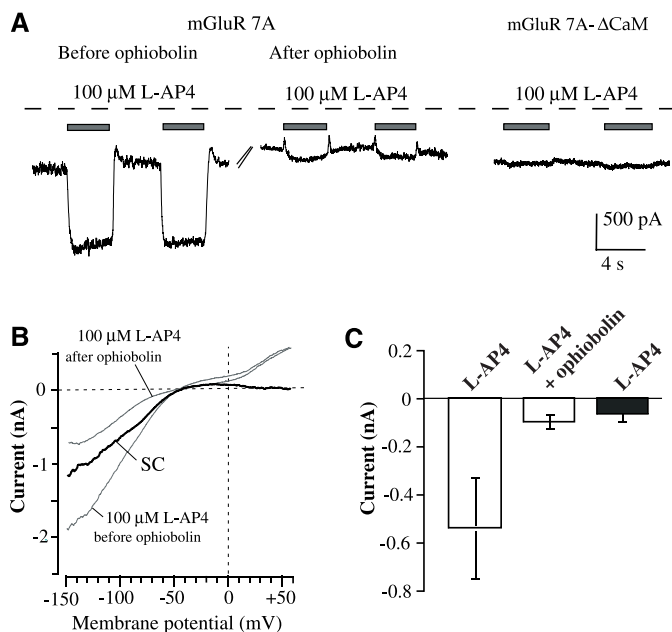
To directly demonstrate that calmodulin binding is critical for mGluR 7 signaling, we generated a mutant 7A- Δ CaM, in which amino acids 864 to 876 (KAVVTAATMSSRL) (26) were deleted from the tail's calmodulin binding site. GST-7A- Δ CaM failed to interact with calmodulin under the conditions de-

scribed previously (8, 12) but bound G $\beta\gamma$ as efficiently as the wild-type receptor (Fig. 2D).

Calmodulin proved unable to compete with binding of G $\beta\gamma$ to this fusion construct (Fig. 2D). Only $6.8 \pm 6.7\%$ of control G β binding was found by densitometry with GST-7A in the presence of Ca $^{2+}$ -calmodulin, whereas GST-7A- Δ CaM bound $90.6 \pm 19\%$ under the same conditions ($n = 3$). We therefore tested a full-length mGluR 7A- Δ CaM construct for functional coupling by coexpression with concatenated pairs of G protein-activated inwardly rectifying Kir channels (27). HEK 293 cells cotransfected with wild-type mGluR 7A and Kir3.1/3.2 generated an inward current of -693 ± 190 pA ($n = 13$) in response to hyperpolarizing voltage

REPORTS

Fig. 4. mGluR 7A coupling to heteromeric Kir3.1/3.2 channels depends on calmodulin. (A) Whole-cell current responses recorded from HEK 293 cells cotransfected with Kir3.1/3.2 subunits and either mGluR 7A or mGluR 7A- Δ CaM, upon superfusion of 100 μ M L-AP4 at a holding potential of -100 mV. Note the rapid activation and inactivation of L-AP4-induced currents. After incubation with ophiobolin A (25 μ M) for 2 min, L-AP4-induced currents of mGluR 7A (left) were greatly suppressed (middle). In cells coexpressing mGluR 7A- Δ CaM, only a very small L-AP4-induced increase in inward current was seen even in the absence of ophiobolin A (right panel). Dashed line indicates zero current level; all recordings were performed in 25 mM external K^+ . (B) Whole-cell current responses to 1-s voltage ramps between -150 and $+60$ mV recorded from cells cotransfected with mGluR 7A and Kir3.1/3.2 in the presence of 100 μ M L-AP4 before and after incubation with ophiobolin A. The thick black trace represents the subtraction current (SC). (C) Kir3.1/3.2 current amplitudes at -100 mV in the presence of 100 μ M L-AP4 before (-546 ± 210 pA) and after a 2-min incubation with 25 μ M ophiobolin A (-106 ± 27 pA; $n = 11$ each) for mGluR 7A (white bars), and without ophiobolin A for mGluR 7A- Δ CaM (black bar).



steps that was prominently enhanced by 100 μ M L-AP4 (-1239 ± 397 pA for Kir3.1/3.2, $n = 13$) (Fig. 4A). In cells responding to L-AP4, the current-voltage relation of basal and agonist-induced currents showed steep voltage dependence with strong rectification typical of I_{kir3} currents (Fig. 4B). Both the onset of current activation by L-AP4 and recovery upon removal of the ligand occurred rapidly with a rate of 2 to 3 s^{-1} , suggesting that the Kir open probability is regulated by mGluR 7A via G $\beta\gamma$. In the presence of ophiobolin A, these L-AP4-induced inward currents declined (Fig. 4, A and B) by $>80\%$.

L-AP4 failed to enhance inward currents in cells coexpressing mGluR 7A- Δ CaM and Kir3.1/3.2 (Fig. 4, A and C). This loss of L-AP4-induced mGluR 7A could not be attributed to impaired membrane targeting of the mutant receptor, because surface immunoreactivities of HEK 293 cells transfected with mGluR 7A and mGluR 7A- Δ CaM were similar (28). Moreover, L-AP4 stimulated the binding of [35 S]GTP- γ -S (29) to membranes prepared from HEK 293 cells transfected with either mGluR 7A or mGluR 7A- Δ CaM to rather similar extents (18). These results show that the calmodulin binding site in the mGluR 7A C-tail is dispensable for G protein activation, but required for G $\beta\gamma$ mediated signaling by group III mGluRs.

Calmodulin is known as a multifunctional element in fine-tuning of transmitter release: Paired pulse facilitation involves Ca^{2+} -cal-

modulin-dependent kinase II (30), after-hyperpolarization via Ca^{2+} -dependent K^+ channels requires calmodulin (31), and Ca^{2+} -dependent inactivation as well as recovery of P/Q-type Ca^{2+} channels is mediated by calmodulin (32). Together, these mechanisms support the efficiency of synaptic transmission. Our data show that calmodulin is also required for autoinhibition of glutamate release, where it promotes dissociation of G $\beta\gamma$ from presynaptic mGluR C-tails, thus making G $\beta\gamma$ available for inhibiting voltage-dependent Ca^{2+} channels (3, 4). This action of calmodulin requires Ca^{2+} . Presynaptic activity will raise both extracellular glutamate necessary for the activation of the low-affinity mGluR 7 and intracellular Ca^{2+} to support calmodulin actions. Therefore, calmodulin regulation of presynaptic mGluRs signaling as described here may contribute to the activity dependence of autoinhibition previously observed at glutamatergic synapses (33).

References and Notes

1. S. M. Thompson, M. Capogna, M. Scanziani, *Trends Neurosci.* **16**, 222 (1993).
2. J.-P. Pin and J. Bockaert, *Curr. Opin. Neurobiol.* **5**, 342 (1995); J.-P. Pin and R. Duvoisin, *Neuropharmacology* **34**, 1 (1995).
3. T. J. Bushnell et al., *Br. J. Pharmacol.* **117**, 1457 (1996); T. Takahashi, I. D. Forsythe, T. Tsujimoto, M. Barnes-Davies, K. Onodera, *Science* **274**, 594 (1996).
4. S. R. Ikeda, *Nature* **380**, 255 (1996); S. Herlitze et al., *ibid.*, p. 258.
5. R. Shigemoto et al., *ibid.* **381**, 523 (1996); R. Shigemoto et al., *J. Neurosci.* **17**, 7503 (1997).

6. J. A. Saugstad, J. M. Kinzie, M. M. Shinohara, T. P. Sergeron, G. L. Westbrook, *Mol. Pharmacol.* **51**, 119 (1997).
7. To generate sequences encoding the COOH-terminal region of mGluR 7 [N. Okamoto et al., *J. Biol. Chem.* **269**, 1231 (1994)], we used oligonucleotides complementary to the codons of amino acids 851 to 857 (HPELVNQ; gagattccacctgaaactcaatgtccag) and 910 to 916 (YNNLVlstop; ctgtcgtactagataaccagggtattata) in a standard PCR on mouse brain cDNA at annealing temperatures of 52°C (26). This generated two products corresponding to cDNAs encoding the known COOH-terminal region of mGluR 7 (mGluR 7A) and a recently reported splice variant [P. J. Flor et al., *Neuropharmacology* **36**, 153 (1997)] containing an additional 81-base pair insertion (mGluR 7B). Full-length mGluR 7A- Δ CaM and truncated mGluR 7A tail sequences were also generated by PCR using a similar procedure. All amplification products were verified by automated DNA sequencing.
8. To produce GST fusion proteins, we subcloned cDNAs into the Eco RI and Sal I sites of pGEX-5X1 before transformation into *E. coli* BL21 (Stratagene). The cytosol of bacteria expressing the GST-fusion proteins was incubated with glutathione-Sepharose for 2 hours at 4°C followed by sequential washes (washes 1 to 3) in binding buffer [BB; 20 mM Hepes, 100 mM KCl (pH 7.4), and protease inhibitor cocktail Complete (Boehringer-Mannheim)], BB containing 0.1% (w/v) Triton X-100, and BB containing 2 mM $MgCl_2$ and 0.5 mM adenosine triphosphate (ATP). Immobilized fusion proteins were then used in binding assays. Cytosolic fractions were obtained from freshly dissected rat brains, and SDS-polyacrylamide gel electrophoresis (PAGE) and protein immunoblotting were performed according to published procedures [L. L. Pellegrini, V. O'Connor, F. Lottspeich, H. Betz, *EMBO J.* **14**, 4705 (1995)]. The fractions (~ 5 mg protein/ml) were dialyzed into BB, cleared by centrifugation, and preadsorbed by incubation for 2 hours at 4°C with GST bound to glutathione-Sepharose 4B (Pharmacia). Aliquots of these fractions were supplemented with 1 mM $CaCl_2$ or 5 mM EGTA (when indicated) and incubated for 2 hours at 4°C with 5 mg of the respective GST fusion protein prebound to glutathione-Sepharose (1 ml). After removal of unbound proteins and washing of the beads in BB containing the appropriate $CaCl_2$ (1 mM) or EGTA (5 mM) supplement, bound proteins were eluted with 15 mM reduced glutathione or SDS-PAGE sample buffer. In binary binding reactions, 20 μ g of immobilized fusion protein (GST-7A) was incubated with 10 μ g calmodulin (Calbiochem) for 2 hours at 4°C in BB supplemented with either $CaCl_2$ or EGTA. After repeated washing, the beads were eluted with SDS-PAGE sample buffer.
9. R. D. Hinrichsen, *Biochim. Biophys. Acta* **1155**, 277 (1993).
10. R. Minkami, N. Jinnai, H. Sugiyama, *J. Biol. Chem.* **272**, 20291 (1997).
11. Affinity measurements were done by fluorescence spectroscopy using dansylated calmodulin.
12. V. O'Connor, O. El Far, J. Airas, unpublished data.
13. P. James, T. Vorherr, E. Carafoli, *Trends Biochem. Sci.* **20**, 38 (1995).
14. P. C. Leung, W. A. Taylor, J. H. Wang, C. L. Tipton, *J. Biol. Chem.* **259**, 2742 (1984).
15. V. O'Connor, unpublished data.
16. Porcine brain membranes (prewashed with EDTA and EGTA, 1 mM each) were extracted in the presence of 10 mM CHAPS (29). Oligomeric G proteins (G_i and G_o , $>80\%$ G_i) were purified from bovine or porcine brain membranes; G $\beta\gamma$ was chromatographically resolved from $G\alpha$ [R. Jockers et al., *J. Biol. Chem.* **269**, 32077 (1994)]. Detergent extracts (containing 100 μ g of protein), or 30 pmol of purified oligomeric G proteins or G $\beta\gamma$, or the indicated amounts of purified recombinant $G\alpha_{i1}$ [S. M. Mumby and M. E. Linder, *Methods Enzymol.* **327**, 254 (1994)], were incubated with 30 μ g of GST, GST-7A, or GST-7A- Δ CaM for 1 hour at 20°C in GBB [G protein binding buffer: 50 mM tris-HCl (pH 8.0), 1 mM EDTA, 150 mM NaCl, 8 mM CHAPS, and 10 μ M guanosine diphosphate] in a total volume of 0.14 ml. After addition of 200 pmol of calmodulin and 2 mM Ca^{2+} , preequilibrated glutathi-

REPORTS

- one-Sepharose 4B beads (20 μ l of a 50% slurry) were added, and incubation continued for 2 hours at 4°C. Ca^{2+} did not affect the binding of $G\beta\gamma$ to GST-7A. After repeated washing, bound proteins were eluted with 30 mM glutathione or SDS sample buffer. Immunoblots were done with antiserum 7 ($G\beta$ -common) or antiserum 11 ($G\alpha$ -common) (29).
17. P. J. Conn and J. P. Pin, *Annu. Rev. Pharmacol. Toxicol.* **37**, 205 (1997).
 18. M. Freissmuth, C. Nanoff, E. Bofill-Cardona, data not shown.
 19. Hippocampi from neonatal Sprague-Dawley rats were dissociated and plated onto micro-islands of glia cells according to published methods (20) [J. M. Bekkers and C. F. Stevens, *Proc. Natl. Acad. Sci. U.S.A.* **88**, 7834 (1991)]. After 10 to 15 days in vitro, autaptic currents were recorded at 20° to 24°C from neuronal somata (20). Neurons were clamped at -70 mV and depolarized for 1 to 2 ms to 0 mV once every 20 s. Stimulation and current recordings were performed with a List EPC-7 amplifier controlled by PClamp 6.0 software (Axon Instruments). Electrodes pulled from borosilicate glass capillaries (Flaming/Brown micropipette puller; Sutter Instruments) were filled with a solution containing 140 mM KCl, 1.6 mM $CaCl_2$, 10 mM EGTA, 10 mM Hepes, 2 mM Mg-ATP, and 2 mM Li-GTP, adjusted to pH 7.3 with KOH. The bathing solution consisted of 140 mM NaCl, 6 mM KCl, 3 mM $CaCl_2$, 2 mM $MgCl_2$, 20 mM glucose, and 10 mM Hepes, adjusted to pH 7.4 with NaOH. Drug application was performed as described (20). Postsynaptic glutamate responses were elicited by the direct application of 100 μ M glutamate.
 20. S. Boehm and H. Betz, *J. Neurosci.* **17**, 4066 (1997).
 21. S. Boehm, data not shown.
 22. S. R. Bradley, A. I. Levey, S. M. Hersch, P. J. Conn, *J. Neurosci.* **16**, 2044 (1996).
 23. N. K. Thomas, D. E. Jane, H. W. Tse, J. C. Watkins, *Neuropharmacology* **35**, 637 (1996).
 24. K. Gietzen, I. Sadorf, H. Bader, *Biochem. J.* **207**, 541 (1982).
 25. K. P. Scholz and R. J. Miller, *Neuron* **8**, 1139 (1992).
 26. Abbreviations for the amino acid residues are as follows: A, Ala; C, Cys; D, Asp; E, Glu; F, Phe; G, Gly; H, His; I, Ile; K, Lys; L, Leu; M, Met; N, Asn; P, Pro; Q, Gln; R, Arg; S, Ser; T, Thr; V, Val; W, Trp; and Y, Tyr.
 27. E. Wischmeyer *et al.*, *Mol. Cell. Neurosci.* **9**, 194 (1997).
 28. O. El Far, unpublished data.
 29. C. Nanoff, T. Mitterauer, F. Roka, M. Hohenegger, M. Freissmuth, *Mol. Pharmacol.* **48**, 806 (1995).
 30. P. F. Chapman, B. G. Frenguelli, A. Smith, C. M. Chen, A. J. Silva, *Neuron* **14**, 591 (1995).
 31. X. M. Xia *et al.*, *Nature* **395**, 503 (1998).
 32. A. Lee *et al.*, *Nature* **399**, 155 (1999).
 33. M. Scanziani, P. A. Salin, K. E. Vogt, R. C. Malenka, R. A. Nicoll, *Nature* **385**, 630 (1997).
 34. We thank R. Shigemoto for mGluR 7A antisera, S. Nakanishi for cDNA, A. Niehuis, A. Motejlek, and E. Wischmeyer for experimental assistance, and M. Baier and H. Reitz for secretarial help. Supported by Deutsche Forschungsgemeinschaft (H.B.), Fonds der Chemischen Industrie (H.B.), the Human Frontier Science Program Organization (HFSP/O: H.B.), and the Austrian Science Foundation (S.B., M.F., and C.N.). O.E.F. was supported by a HFSP/O postdoctoral fellowship, and E.B.C. by a grant from the European Community.

23 July 1999; accepted 30 September 1999

Enhance your AAAS membership with the Science Online advantage.



All the information you need... in one convenient location.

Visit Science Online at <http://www.scienceonline.org>, call 202-326-6417, or e-mail membership2@aaas.org for more information.

AAAS is also proud to announce site-wide institutional subscriptions to Science Online. Contact your subscription agent or AAAS for details.

Science ONLINE



Full text Science—research papers and news articles with hyperlinks from citations to related abstracts in other journals before you receive *Science* in the mail.



ScienceNOW—succinct, daily briefings, of the hottest scientific, medical, and technological news.



Science's Next Wave—career advice, topical forums, discussion groups, and expanded news written by today's brightest young scientists across the world.



Research Alerts—sends you an e-mail alert every time a *Science* research report comes out in the discipline, or by a specific author, citation, or keyword of your choice.



Science's Professional Network—lists hundreds of job openings and funding sources worldwide that are quickly and easily searchable by discipline, position, organization, and region.



Electronic Marketplace—provides new product information from the world's leading science manufacturers and suppliers, all at a click of your mouse.



AMERICAN ASSOCIATION FOR THE
ADVANCEMENT OF SCIENCE